

Ga-doped ZnO single-crystal nanotips grown on fused silica by metalorganic chemical vapor deposition

J. Zhong, S. Muthukumar, Y. Chen, and Y. Lu^{a)}

School of Engineering, Rutgers University, Piscataway, New Jersey 08854-8058

H. M. Ng

Lucent Technologies, 600 Mountain Avenue, Murray Hill, New Jersey 07974

W. Jiang and E. L. Garfunkel

Department of Chemistry, Rutgers University, Piscataway, New Jersey 08854-8087

(Received 8 April 2003; accepted 29 August 2003)

In situ Ga-doped ZnO nanotips were grown on amorphous fused silica substrates using metalorganic chemical vapor deposition. Structural, optical, and electrical properties of as-grown ZnO nanotips are investigated. Despite the amorphous nature of fused silica substrates, Ga-doped ZnO nanotips are found to be single crystalline and oriented along the *c*-axis. Photoluminescence (PL) spectra of Ga-doped ZnO nanotips are dominated by near-band-edge emission with negligible deep-level emission. The increase in PL intensity from Ga doping has been attributed to the increase of Ga donor-related impurity emission. Current–voltage characteristics of the ZnO nanotips are measured by conductive-tip atomic force microscopy, which shows the conductivity enhancement due to Ga doping. © 2003 American Institute of Physics. [DOI: 10.1063/1.1621729]

ZnO is a wide-band-gap semiconductor that is currently undergoing a renaissance because of its many exciting properties. ZnO has a high exciton binding energy (60 meV). Excitonic emission, in contrast to electron–hole plasma recombination, leads to a low lasing threshold in ZnO. Enhanced carrier and photon confinement in ZnO nanowires have enabled the demonstration of an optically addressed ZnO nanolaser at room temperature.¹ Recently, field emission from ZnO nanowires has also been reported.^{2,3} ZnO nanotips are attractive for field-emission displays due to their low emission barrier, high saturation velocity, and high radiation hardness.

A variety of techniques have been exploited to grow ZnO nanowires, such as template-assisted growth,⁴ solution-based synthesis,⁵ vapor–liquid–solid methods,¹ catalyst-driven molecular-beam epitaxy,⁶ chemical vapor deposition (CVD),⁷ metalorganic vapor phase epitaxy (MOVPE),⁸ and metalorganic chemical vapor deposition (MOCVD).⁹ Among these methods catalyst-free growth using MOCVD offers the capability of large-scale mass production, selective growth, and compatibility with other well-developed semiconductor processing technologies. ZnO nanowires grown on *c*-sapphire using MOVPE have shown promising optical properties of free-excitonic emission at 10 K.⁸ In comparison with most single-crystal substrates, amorphous substrates such as fused silica/glass are of particular interest due to their low cost. Furthermore, controllable *in situ* doping of single-crystal semiconductor nanostructures is critical to realize nanoscale electronic and photonic devices. Selective doping in InP nanowires has been exploited to produce nanoscale *p*–*n* junctions.¹⁰ Enhanced field emission has been demonstrated in boron-doped carbon nanotubes due to the change in density of states near the Fermi level created by the dopant

atoms that leads to a reduced work function.¹¹ Conductivity enhancement is also observed in boron-doped Si nanowires by using scanning tunneling spectroscopy.¹² In this letter, we report the MOCVD growth and *in situ* *n*-type Ga-doping of ZnO single-crystal nanotips on fused silica substrates. Structural, optical, and electrical properties of the ZnO nanotips with and without Ga-doping are studied.

ZnO nanotips with different Ga doping levels were grown on fused silica substrates using a vertical flow MOCVD system. Diethylzinc, oxygen, and triethylgallium were used as the Zn metalorganic source, oxidizer, and Ga metalorganic sources, respectively. The growth temperature of ZnO nanotips was in the range of 300 to 500 °C. Ga/Zn mole ratio was altered from 10^{−4} to 10^{−2} during the Ga-doped ZnO film growth. Details of the ZnO nanotip growth using MOCVD have been described elsewhere.⁹ Epitaxial ZnO films, which were simultaneously grown on (01 $\bar{1}2$) *r*-sapphire¹³ substrates, serve as reference samples for doping information in ZnO nanotips. The resistivities of the epi-ZnO films were characterized using the four-point-probe method. Figure 1(a) shows the measured resistivities of Ga-doped epitaxial ZnO films versus Ga/Zn mole ratios. A Leo–Zeiss field-emission scanning electron microscope (FESEM) was used to characterize the morphology of the films and a Topcon 002B transmission electron microscope (TEM) was used to perform detailed structural characterizations. Photoluminescence (PL) spectra were excited with a 325 nm He–Cd laser. An optical cryostat was used in the 77 K PL measurement.

Shown in Fig. 1(b) is a FESEM image of Ga-doped ZnO nanotips grown on a fused silica substrate. Inset (c) shows the top view of the ZnO nanotips. The diameter of the bottom of nanotips is in the range of 40 to 60 nm and the height is ~850 nm, giving an aspect ratio of ~17:1. Shown in Fig. 2(c) is a dark-field TEM image of the Ga-doped ZnO nanotip along the [2 $\bar{1}10$] zone axis. The selected area electron dif-

^{a)}Author to whom correspondence should be addressed; electronic mail: ylu@ece.rutgers.edu

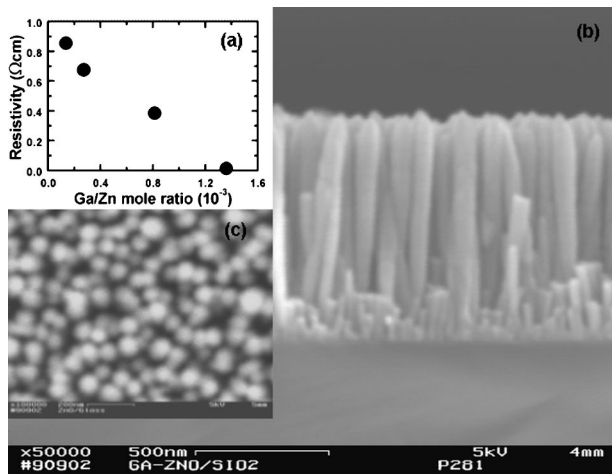


FIG. 1. (a) Measured resistivity of Ga-doped epitaxial ZnO films versus Ga/Zn mole ratios. (b) FESEM image of Ga-doped ZnO nanotips grown on fused silica substrate. (c) Top view of the ZnO nanotips.

fraction and the high-resolution images are shown in insets (a) and (b), respectively. Electron microscopy confirms the single-crystal quality of the Ga-doped ZnO nanotips. High-resolution lattice images show a single-crystalline nanoscale tip. We do not observe any significant structural change between undoped and Ga-doped ZnO nanotips.

Under certain growth conditions, ZnO grown on various substrates shows a columnar structure with rods ending in tips.⁹ Columnar growth is usually considered to result from a high growth rate along the c -axis of ZnO. ZnO is a polar semiconductor, with (0001) planes being Zn terminated and (000 $\bar{1}$) planes being O terminated. These two crystallographic planes have opposite polarity, and hence have different surface energies.¹⁴ The initial ZnO crystals that nucleate on the amorphous fused silica surface presumably do not have a specific epitaxial arrangement, resulting in randomly oriented nuclei. A columnar structure may result from either competitive blocking of all crystallites whose c -axis is pointing away from the surface normal, or a preferential orienta-

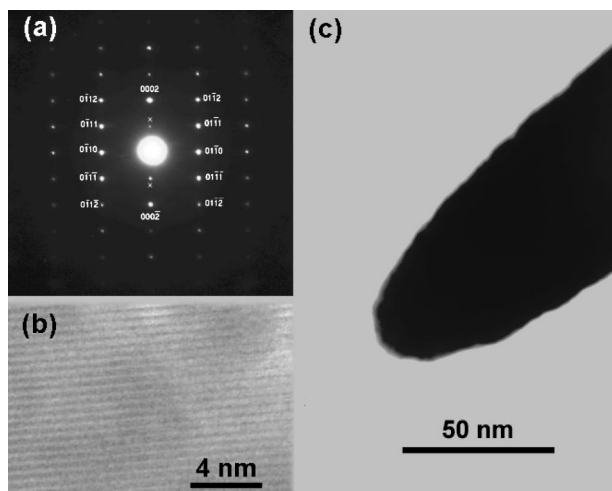


FIG. 2. (a) Selected area diffraction pattern of a single Ga-doped ZnO nanotip along the $[2\bar{1}10]$ zone axis, (b) an image of a single-crystalline tip from high-resolution TEM, and (c) dark-field TEM image of a single Ga-doped ZnO nanotip.

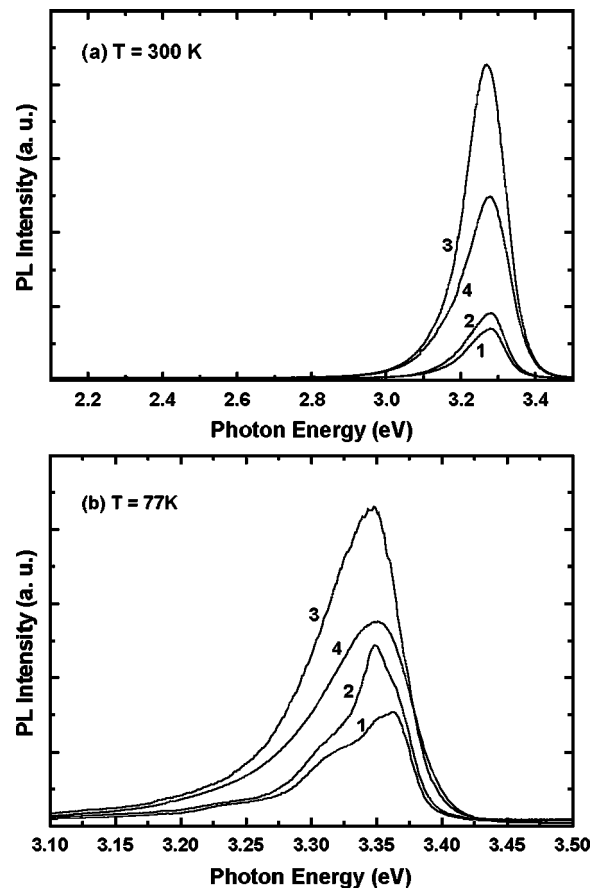


FIG. 3. (a) RT PL spectra of undoped and Ga-doped ZnO nanotips. (b) 77 K PL spectra of undoped and Ga-doped ZnO nanotips. Curves 1, 2, 3, and 4 correspond to the spectra of undoped and Ga-doped ZnO nanotips with reference resistivities of $40\ \Omega\text{ cm}$ (undoped), $0.58\ \Omega\text{ cm}$ (Ga-doped), $4.0 \times 10^{-3}\ \Omega\text{ cm}$ (Ga-doped) and $3.0 \times 10^{-3}\ \Omega\text{ cm}$ (Ga-doped), respectively.

tion of the ZnO nuclei on the relatively flat SiO_2 surface once they reach some critical size.

Figure 3(a) shows the RT PL spectra of undoped and Ga-doped ZnO nanotips. Curve 1 is for the undoped ZnO nanotips with a reference resistivity ρ_{ref} of $40\ \Omega\text{ cm}$, curves 2, 3, and 4 correspond to Ga-doped ZnO nanotips with ρ_{ref} of 0.58 , 4.0×10^{-3} , and $3.0 \times 10^{-3}\ \Omega\text{ cm}$, respectively. It has been reported that due to excess exciton impurity and crystalline defect scattering, there exists a deep-level emission around $2.4\ \text{eV}$ in the undoped ZnO nanowires or whiskers.^{4,15} The almost negligible deep-level emission in Fig. 3(a) suggests good optical quality of the Ga-doped ZnO nanotips. For ZnO nanotips, the near-band-edge (NBE) recombination that monotonically increases with ρ_{ref} is decreased to $4 \times 10^{-3}\ \Omega\text{ cm}$ upon progressively increasing Ga doping [curves 1, 2, and 3 in Fig. 3(a)]. With a further increase in the Ga doping level, the peak intensity starts to decrease [curve 4 in Fig. 3(a)]. Half-width broadening can be seen in the spectra when ρ_{ref} is at $4 \times 10^{-3}\ \Omega\text{ cm}$ or less [curves 3 and 4 in Fig. 3(a)]. Figure 3(b) shows the 77 K PL spectra of the same set of samples. At 77 K, undoped ZnO nanotips (curve 1) display a dominant NBE emission around $3.36\ \text{eV}$, which lies in the spectral range of multiple emission lines associated with neutral donor bound-exciton recombination.¹⁶ We speculate that the NBE emission may arise from bound-exciton emission involving donor-like complexes.¹⁷

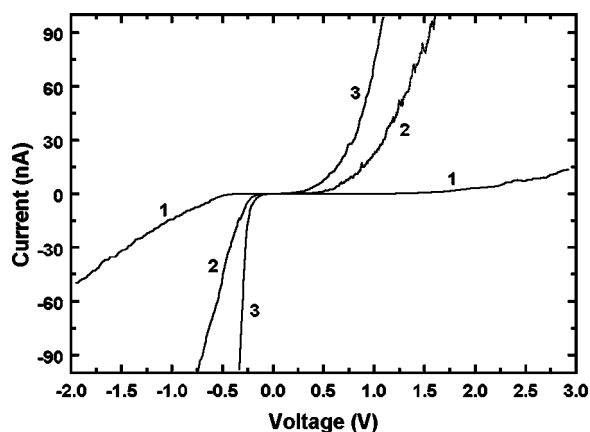


FIG. 4. I - V spectra for the undoped and Ga-doped ZnO nanotips, where curves 1, 2, and 3 correspond to the spectra of undoped and Ga-doped ZnO nanotips with reference resistivities of 40 Ω cm (undoped), 0.58 Ω cm (Ga-doped), 4.0×10^{-3} Ω cm (Ga-doped), respectively.

We also note that two weak shoulders appear on the low-energy tail of the dominant 3.36 eV peak. These shoulders disappear gradually with Ga incorporation giving rise to a new emission line around 3.35 eV that dominates the spectra. This 3.35 eV emission line shows the same trend as the main peak at RT in terms of the intensity and half-width versus doping. Such doping-related behavior has been reported in low-temperature PL spectra of Ga-doped ZnO epitaxial films,^{18,19} where a Ga donor bound-exciton complex has been proposed to be responsible for the increase of PL intensity from Ga doping. Figure 3(b) suggests the 3.35 eV peak could be related to the Ga donor in view of its contribution to the NBE emission. Therefore, at low or moderate Ga doping levels, the increase of PL intensity is primarily caused by the increase of the impurity emission presumably due to an increased Ga dopant concentration. In heavily Ga-doped ZnO nanotips, the competition between the two processes, that is, radiative and nonradiative transitions, becomes prominent. Excess Ga atoms can create nonradiative recombination centers, such as impurity complexes likely involving native defects, or impurity-assisted nonradiative transition channels, resulting in a reduction of the NBE luminescence. As the 3.35 eV peak follows the same half-width versus doping trend as observed at RT, the linewidth broadening in Ga-doped ZnO nanotips might result from potential fluctuations in the nanostructures that arise from random microscopic distribution of the dopants.

Conductive-tip atomic force microscopy (C-AFM) is another useful method to explore nanoscale electrical characteristics in nanoscale materials. In this work, I - V spectra were taken at RT using a JEOL vacuum scanning-tunneling-microscope/AFM system that was operated in a C-AFM mode. Multiple I - V spectra on different ZnO nanotips as well as calibration experiments were performed to ensure reproducibility. Figure 4 shows the tunneling I - V spectra for both undoped and Ga-doped ZnO nanotips. Curves 1, 2, and

3 correspond to the spectra of undoped and Ga-doped ZnO nanotips with ρ_{ref} of 40 Ω cm (undoped), 0.58 Ω cm (Ga-doped), 4.0×10^{-3} Ω cm (Ga-doped), respectively. The asymmetry in the rising slopes of the conduction and valence bands show that the "undoped" ZnO nanotips are intrinsically n -type, in agreement with the observations in the as-grown epitaxial ZnO films. Significantly steeper rising slopes in I - V spectra are clear in Ga-doped ZnO nanotips (curves 2 and 3) in comparison with those in the undoped nanotips (curve 1). These confirm the conductivity enhancement in ZnO nanotips due to Ga doping.

In summary, we have demonstrated fabrication of *in situ* Ga-doped ZnO nanotips grown on amorphous fused silica substrates by MOCVD. ZnO nanotips are shown aligned along the c -axis. TEM measurements confirm the ZnO nanotips are single crystals with no observable structural change from Ga doping. Ga-doped ZnO nanotips possess good optical properties with negligible deep level emission in PL spectra. Nanoscale tunneling I - V spectra exhibit conductivity enhancement due to Ga doping. The conductivity-tailoring achieved in Ga-doped ZnO nanotips opens up possibilities for the fabrication of novel nanoscale devices.

This work has been supported by National Science Foundation under the grants CCR-0103096 and ECS-0088549.

- ¹ M. H. Huang, S. Mao, H. Feick, H. Q. Yan, Y. Y. Wu, H. Kind, E. Weber, R. Russo, and P. D. Yang, *Science* **292**, 1897 (2001).
- ² C. J. Lee, T. J. Lee, S. C. Lyu, Y. Zhang, H. Ruh, and H. J. Lee, *Appl. Phys. Lett.* **81**, 3648 (2002).
- ³ L. Dong, J. Jiao, D. W. Tuggle, J. M. Petty, S. A. Elliff, and M. Coulter, *Appl. Phys. Lett.* **82**, 1096 (2003).
- ⁴ Y. Li, G. W. Meng, L. D. Zhang, and F. Phillipp, *Appl. Phys. Lett.* **76**, 2011 (2000).
- ⁵ L. Vayssieres, *Adv. Mater. (Weinheim, Ger.)* **15**, 464 (2003).
- ⁶ Y. W. Heo, V. Varadarajan, M. Kaufman, K. Kim, D. P. Norton, F. Ren, and P. H. Fleming, *Appl. Phys. Lett.* **81**, 3046 (2002).
- ⁷ J. Wu and S. Liu, *J. Phys. Chem. B* **106**, 9546 (2002).
- ⁸ W. I. Park, Y. H. Jun, S. W. Jung, and G.-C. Yi, *Appl. Phys. Lett.* **82**, 964 (2003).
- ⁹ S. Muthukumar, H. Sheng, J. Zhong, Z. Zhang, N. W. Emanetoglu, and Y. Lu, *IEEE Trans. Nanotechnol.* **2**, 50 (2003).
- ¹⁰ X. Duan, Y. Huang, Y. Cui, J. Wang, and C. M. Lieber, *Nature (London)* **409**, 66 (2001).
- ¹¹ J. C. Charlier, M. Terrones, M. Baxendale, V. Meunier, T. Zacharia, N. L. Rupesinghe, W. K. Hsu, N. Grobert, H. Terrones, and G. A. J. Amaratunga, *Nano Lett.* **2**, 1191 (2002).
- ¹² D. D. Ma, C. S. Lee, and S. T. Lee, *Appl. Phys. Lett.* **79**, 2468 (2001).
- ¹³ C. R. Gorla, W. E. Mayo, S. Liang, and Y. Lu, *J. Appl. Phys.* **87**, 3736 (2000).
- ¹⁴ P. W. Tasker, *J. Phys. C* **12**, 4977 (1979).
- ¹⁵ J. Q. Hu and Y. Bando, *Appl. Phys. Lett.* **82**, 1401 (2003).
- ¹⁶ H. J. Ko, Y. F. Chen, T. Yao, K. Miyajima, A. Yamamoto, and T. Goto, *Appl. Phys. Lett.* **77**, 537 (2000).
- ¹⁷ D. C. Reynolds, D. C. Look, B. Jogai, C. Litton, T. C. Collins, W. Harsch, and G. Cantwell, *Phys. Rev. B* **57**, 12 151 (1998).
- ¹⁸ H. J. Ko, Y. F. Chen, S. K. Hong, H. Wensch, T. Yao, and D. C. Look, *Appl. Phys. Lett.* **77**, 3761 (2000).
- ¹⁹ H. Kato, M. Sano, K. Miyamoto, and T. Yao, *J. Cryst. Growth* **237-239**, 538 (2002).